RESEARCH ARTICLE

WILEY

Establishment of a non-integrated induced pluripotent stem cell line derived from human chorionic villi cells

Ping Long[1,2,3,4] | Yuechuan Shi[1,2,3,5] | Fei Sun[1,2,3,6] | Yunjian Wei[1,2,3] | Bangyong Wu[1,2,3] | Qi Li[1,2,3] | Qiuling Jie[1,2,3] [ID] | Yanlin Ma[1,2,3,5] [ID]

[1]Hainan Provincial Key Laboratory for Human Reproductive Medicine and Genetic Research, The First Affiliated Hospital of Hainan Medical University Haikou, Haikou, Hainan, China

[2]Key Laboratory of Tropical Translational Medicine of Ministry of Education, Hainan Medical University, Haikou, Hainan, China

[3]Haikou Key Laboratory of Human Genetic Resources Preservation of First Affiliated Hospital, Hainan Medical University, Haikou, Hainan, China

[4]Guizhou Qiannan People's Hospital, Guizhou, China

[5]Hainan Medical University, Haikou, Hainan, China

[6]Department of Obstetrics and Gynecology of Nanfang Hospital, Southern Medical University, Guangzhou, China

Correspondence
Yanlin Ma and Qiuling Jie, Hainan Provincial Key Laboratory for Human Reproductive Medicine and Genetic Research, The First Affiliated Hospital of Hainan Medical University, Hainan Medical University, 3 Xueyuan Road, Haikou, Hainan, China.
Emails: mayanlinma@hotmail.com (Y. M.); 990502727@qq.com (Q. J.)

Abstract

Background: Few studies have investigated the generation of induced pluripotent stem cells (iPSCs) derived from human primary chorionic villi (CV) cells. The present study aimed to explore an optimal electroporation (EP) condition for generating non-integrated iPSCs from CV cells (CV-iPSCs).

Methods: The EGFP plasmid was transfected into CV cells under different EP conditions to evaluate cell adherence and the rate of EGFP positive cells. Subsequently, CV cells were transfected with the pEP4-E02S-ET2K and pCEP4-miR-302–367 plasmids under optimal EP conditions. Finally, CV-iPSC pluripotency, karyotype analysis, and differentiation ability were investigated.

Results: Following EP for 48 h under different conditions, different confluency, and transfection efficiency were observed in CV cells. Higher cell density was observed in CV cells exposed to 200 V for 100 s, while higher transfection efficiency was obtained in cells electroporated at a pulse of 300 V for 300 s. To generate typical primitive iPSCs, CV cells were transfected with pEP4-E02S-ET2K and pCEP4-miR-302–367 plasmids using EP and were then cultured in induction medium for 20 days under selected conditions. Subsequently, monoclonal iPSCs were isolated and were evaluated pluripotency with AP positive staining, the expression of OCT4, SOX2, and NANOG in vitro and the formation of three germ layer teratomas in vivo.

Conclusion: CV-iPSCs were successfully established under the conditions of 100 μl shock cup and EP pulse of 200 V for 300 s for two times. This may provide a novel strategy for investigating the pathogenesis of several diseases and gene therapy.

Ping Long and Yuechuan Shi are co-first authors and contributed equally to this work.

1 | INTRODUCTION

In 2006, Yamanaka et al. used reprogramming technology to induce the transformation of murine and human fibroblasts into a type of stem cells that maintained their self-renewal ability and exhibited multidirectional differentiation potential. These cells are widely known as pluripotent stem cells (PSCs), also called induced pluripotent stem cells (iPSCs).[1,2] iPSCs mimic human embryonic stem cells (ESCs) in morphology and function and both cell types exhibit pluripotent differentiation ability, which makes them easy to differentiate into several cell types and tissues. Compared with ESCs, iPSCs can directly enter into the state of PSCs from somatic cells. Furthermore, since there are several sources and simple ways to isolate iPSCs, it is easy to obtain iPSCs with specific genotypes even from the patients themselves, without ethical dilemmas. To date, fibroblasts and keratinocytes from the skin,[2,3] adipose-derived stem cells,[4] peripheral blood cells,[5] amniotic fluid,[6] urine cells,[7] and extra-embryonic tissues such as the placenta, umbilical cord, and amniotic mesenchymal stem cells[8,9] have been successfully used to generated iPSCs.

However, the number of reports on iPSCs derived from human primary chorionic villi (CV) cells is limited and these reports are mainly focus on the generation of lentiviral- or retroviral-induced iPSCs.[10-13] Due to the random insertion of viral genes into the cell genome, the risk of genome integration is high.[14,15] Therefore, non-integrated iPSCs are considered to be the future trend of stem cell applications and regenerative medicine, since the risk of integrating foreign genes is limited. Transfection by electroporation (EP) acts via enhancing cell membrane permeability in a solution under a transient strong electric field, thus promoting the introduction of charged foreign substances into the cells. EP offers several advantages, including versatile application, low cytotoxicity, and simple operation, compared with other transfection methods.[16] Furthermore, EP can be used to transfect cells with different molecules such as DNA and RNA fragments, plasmids, and recombinant proteins, by utilizing a single apparatus.[17] Additionally, EP limits the risk of gene integration to obtain non-integrated iPSCs.[18] However, during EP, the voltage of the electric pulses and the duration of the electric shock are important factors that can affect the transfection efficiency and the energy of the electric field. Therefore, excessive electric field energy can reduce cell survival due to cell membrane destruction. The higher the voltage pulses and the longer the duration, the greater the damage to the cells. Currently, there is no efficient method for transforming human CV cells into non-integrated iPSCs.

The present study aimed to explore the optimal EP conditions for transfecting human CV cells to generate non-integrated iPSCs, thus providing novel insights into stem cell research and regenerative medicine.

2 | METHODS AND MATERIALS

2.1 | Separation and culture of chorionic villi cells

The CV tissues used in the current study were isolated from abortion or prenatal diagnostic specimens at the Reproductive Center and the Prenatal Diagnosis Center of the First Affiliated Hospital of the Hainan Medical University. All patients participated voluntarily in the current study and provided signed informed consent. The study protocol was approved by the Ethics Committee of the First Affiliated Hospital of the Hainan Medical University. The CV tissues were obtained using B-ultrasound-guided puncture under aseptic conditions and were isolated with ophthalmic forceps on a sterile clean bench. Maternal tissues and blood clots were discarded. Subsequently, the isolated CV tissues were digested into a single cell suspension using 0.25% trypsin-EDTA solution and collagenase I. Cells were washed twice with PBS, the cell pellet was retained and then resuspended in CHANG Amnio™ medium (Irvine Scientific, Inc.). Finally, cells were cultured at 37°C in a humidified incubator with 5% CO_2.

2.2 | Exploration of electric transfer conditions

To obtain a stable and efficient induction system, three conditions with optimized voltage pulse and shock duration were set up, according to the manufacturer's instructions (Multiporator®; Eppendorf). The EP conditions were as follows: (i) 200 V pulse for 100 μs, two electric shocks; (ii) 200 V pulse for 300 μs, two electric shocks; and (iii) 300 V pulse for 300 μs, two electric shocks. The electroporator modes were set up for eukaryotic cells, while CV cells at passage two were used for subsequent experiments. CV cells were first digested with 0.25% trypsin-EDTA solution, centrifuged and resuspend in DPBS (Gibco, Inc.) at a density of 1.2 x 10^6 cells/ml. Subsequently, the cell suspension was supplemented with 5 μg EGFP plasmid (Addgene, Inc.) and mixed thoroughly. Transfection was carried out according to the EP conditions set above. Following EP, the cells were seeded into a 6-well plate and cultured at 37°C in a humidified incubator with 5% CO_2. The cell survival rate and the expression levels of the green fluorescent protein were measured at 48 h following transfection.

2.3 | Generation of iPSCs from chorionic villi cells (CV- iPSCs)

Chorionic villi cells at passage two (P2) were resuspend in DPBS at a density of 1.2 x 10^6 cells/ml. Subsequently, the cell suspension was supplemented with 6 μg pEP4-E02S-ET2K (Addgene, Inc.) and 4 μg pCEP4-microRNA(miR)-302–367 (donated by Guangzhou Institutes of Biomedicine and Health, Chinese Academy of Sciences), followed

by thorough mixing. Plasmid pEP4-E02S-ET2K carries three transcription factors, OCT4, SOX2 and KLF4, as well as plasmid marker genes such as oriP, EBNA-1 and SV40, and pCEP4-miR-302–367 carries miR-302, oriP, and EBNA-1. The cell transfection was carried out by EP as described above. CV cells were seeded into a 6-well plate pre-coated with Matrigel™ (BD Biosciences) in 2 ml CHANG Amnio™ medium (FUJIFILM Irvine Scientific, Inc.) and maintained at 37°C in a humidified incubator with 5% CO_2. Following incubation for 24 h, the CHANG Amnio™ medium was replaced in well-adhered cells. When cells reached ~40% confluency, the medium was replaced with mTeSR™1 induction medium (Stemcell Technologies, Inc.) supplemented with four small molecule inhibitors (4i), namely 0.5 μmol/L A-83–01, 0.5 μmol/L thiazovivin, 3 μmol/L CHIR99021, and 1 μmol/L PD0325901. The induction medium was changed every day. When 5–8 colonies with typical ESC-like compact morphology were formed, the mTeSR™1 induction medium was replaced with mTeSR™1 maintenance medium (Stemcell Technologies, Inc.).

2.4 | Selection, purification, and subculture of CV-iPSCs

When ESC-like colonies were formed, occupying the 1/2 of view of the low-power inverted microscope, cells with high nuclear to cytoplasmic ratio, tightly arranged and with smooth and clear edges were picked out under a stereo microscope using the mechanical segmentation method. The above cells were seeded into culture dishes pre-coated with Matrigel™ in mTeSR™1 medium. For purification, cell clones in the early passage were isolated using the mechanical segmentation method. At a later stage, when few differentiated cells covering the 50%–80% of the well dish were observed, these cells were digested with 0.5 mM EDTA and were then inoculated into culture dishes pre-coated with Matrigel™ at a ratio of 1:3 for further expansion. Alternatively, cells were stored at −80°C in a controlled freezer for further use.

2.5 | Alkaline phosphatase staining

Following cell isolation, the remaining cell clones were stained with alkaline phosphatase (AP) staining. Briefly, the old medium was aspirated, cells were washed twice with PBS and fixed with 4% paraformaldehyde (PFA) for 30 min at room temperature. Subsequently, PFA was removed, the cells were washed twice with TBS-Tween-20 (TBST) and equilibrated with 2 ml AP buffer for 5 min at room temperature. Cells were then stained with 1.5 ml AP color developing solution for 30 min in dark. Following incubation, the solution was removed, and cells were washed twice with PBS and observed under an inverted microscope.

2.6 | Immunofluorescence staining to detect the expression levels of iPSC pluripotency-related markers

When cell density reached ~60%, the cells were washed twice with PBS and fixed with 4% PFA for 30 min at room temperature. After PFA was removed, the cells were washed again twice with PBS and permeated with 0.2% Triton X-100 for 30 min at room temperature. Following blocking with 5% BSA for 1 h at room temperature, cells were incubated with primary antibodies diluted in 5% BSA (dilution, 1:200) at 4°C overnight. The following primary antibodies were used in the current study: Anti-octamer-binding transcription factor 4 (OCT4; cat. no. ab19857), anti-stage-specific embryonic antigen-4 (SSEA4; cat. no. ab16287; both from Abcam), anti-TRA-1–60 (cat. no. MAB4360), and anti-TRA-1–81 (cat. no. MAB4381; both from MilliporeSigma). The next day, the cells were washed thrice with PBST followed by incubation with the corresponding secondary antibodies (dilution, 1:1000 in PBST) for 1 h at room temperature in the dark. Following washing thrice with PBST, a DAPI solution was used to stain cell nuclei for 5 min in the dark. After DAPI solution was removed, the wells were rinsed twice with PBS, and the fluorescence-stained cells were observed under a fluorescence microscope (BX51 system microscope; Olympus Corporation).

2.7 | Reverse transcription-quantitative PCR (RT-qPCR)

Untransfected primitive CV cells and iPSCs at passage five were collected, and total RNA was extracted using a TRIzol® reagent (cat. no. 15596018; Invitrogen, Thermo Fisher Scientific, Inc.). Subsequently, total RNA was reverse transcribed into cDNA according to the manufacturer's instructions. RT-qPCR was carried out using the SYBR® Premix Ex Taq TM II kit (cat. no. RR820A; Takara Bio, Inc.) on the Agilent Mx3000P system (Mxpro-Mx3000P; Agilent Technologies, Inc.). The thermocycling conditions used were as follows: 95°C for 5 min, followed by 40 cycles at 95°C for 40 s, 60°C for 30 s, and 72°C for 30 s, and finally 72°C for 7 min. The primer sequences of sex-determining region Y-box 2 (SOX2), OCT4, NANOG, and GAPDH are listed in Table 1.

2.8 | Karyotype analysis

The cytogenetic chromosome analysis of CVcells and CV-iPSCs were performed using the protocol provided by the International System for Human Cytogenomic Nomenclature 2016 (ISCN 2016). For each sample, 20 cells were counted under a microscope and scanning was carried out on a chromosome automatic scanning analysis system.

2.9 | Non-integration analysis

The genomic DNA of P2 CV cells, P11 CV-iPSCs, and CV cells on day 3 after electroporation were extracted using TIANamp Genomic DNA kit (cat. no. DP304-02, TIANGEN, Inc.) according to the manufacturer's protocol. Exogenous gene fragments was amplified by PCR (see Table 1 for PCR primer sequences), then using 1% agarose

TABLE 1 Sequence of gene primers

| Gene name	Forward primer	Reverse primer	Application
SOX2	CCCAGCAGACTTCACATGT	CCTCCCATTTCCCTCGTTTT	RT-qPCR
OCT4	CCTCACTTCACTGCACTGTA	CAGGTTTTCTTTCCCTAGCT	
NANOG	TGAACCTCAGCTACAAACAG	TGGTGGTAGGAAGAGTAAAG	
GAPDH	GGTGCTGAGTATGTCGTGGA	CCTTCCACAATGCCAAAGTT	
OriP	TTCCACGAGGGTAGTGAACC	TCGGGGGTGTTAGAGACAAC	PCR
EBNA–1	ATCGTCAAAGCTGCACACAG	CCCAGGAGTCCCAGTAGTCA	
miR–302–367	TTTCCAAAATGTCGTAATAACCCCG	CTCCCAAAGAGTCCTGTTCTGTCCT	
OCT4	AGTGAGAGGCAACCTGGAGA	AGGAACTGCTTCCTTCACGA	
SOX2	ACCAGCTCGCAGACCTACAT	CCCCCTGAACCTGAAACATA	
KLF4	CCCACACAGGTGAGAAACCT	CCCCCTGAACCTGAAACATA	
GAPDH	GTGGACCTGACCTGCCGTCT	GGAGGAGTGGGTGTCGCTGT	
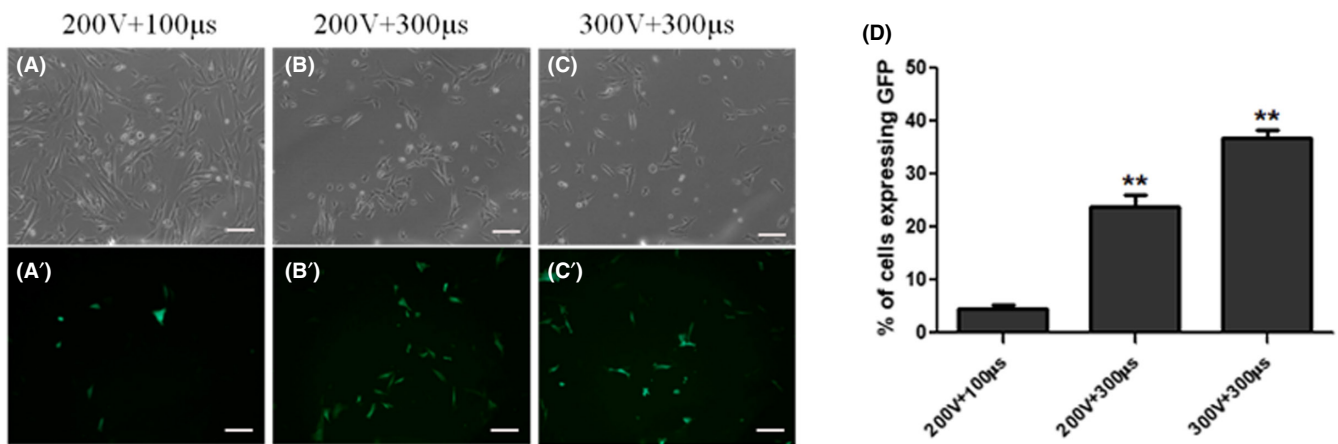
FIGURE 1 Cell status and the positive of GFP (x100, 48 h). (A-C) The adherent state of CV cells after 48 h of electroporation under three different conditions. (A'-C') The positive of GFP protein in CV cells after 48 h of electroporation under three different conditions. (D). Transfection efficiency under three different conditions, **$p < 0.01$

gel electrophoresis to detect PCR products. PCR amplification system used were as follows: Taq-HS PCR Forest Mix (2X) (cat. no. EG15141, Yugong Biolabs, Inc.) for 12.5 μl, forward and reverse each primer for 0.5 μl, DNA for 500 ng/25 μl, ddH2O was supplemented to 25 μl. The PCR amplification program used were as follows: pre-denaturation at 94℃ for 5 min, denaturation at 94℃ for 10 s, annealing at 60℃ for 30 s, extension at 68℃ for 1 min, a total of 35 cycles, and a final extension at 72℃ for 5 min. The ddH$_2$O and P2 CV cells were used as negative controls, and the genomic DNA of CV cells of D3 after electroporation was used as positive control.

2.10 | Teratoma formation

For in vivo differentiation, iPSCs were seeded into a 6-well plate pre-coated with Matrigel™. When reached 70%–80% confluency, cells were digested with dispase, resuspended in Matrigel™ solution diluted in DMEM/F12 at a ratio of 1:3 and were immediately subcutaneously injected into NOD-SCID mice. After 4–6 weeks, when the developed teratomas reached a critical volume of >1 cm^3, the

mice were sacrificed, and teratomas were isolated. Subsequently, teratomas were embedded in paraffin and stained with hematoxylin and eosin (HE). Typical cells in the inner, middle, and outer germ layers were analyzed under a microscope. The study protocol was approved by the Ethics Committee of the Hainan Medical University.

3 | RESULTS

3.1 | Cell morphology and GFP protein expression after transfection under different EP conditions

CV cells transfected using EP under three different conditions were all adhered at 48 h. All cells exhibited a short spindle-shaped morphology with different confluency (Figure 1A-C, and A'-C'). The cell confluency in the 200 V + 100 μs, 200 V + 300 μs, and 300 V + 300 μs groups were ~50%, 30%, and 10%, respectively. The transfection efficiency (GFP positive cells/total adhered cells) in the 300 V + 300 μs group was 36.9%, which was significantly
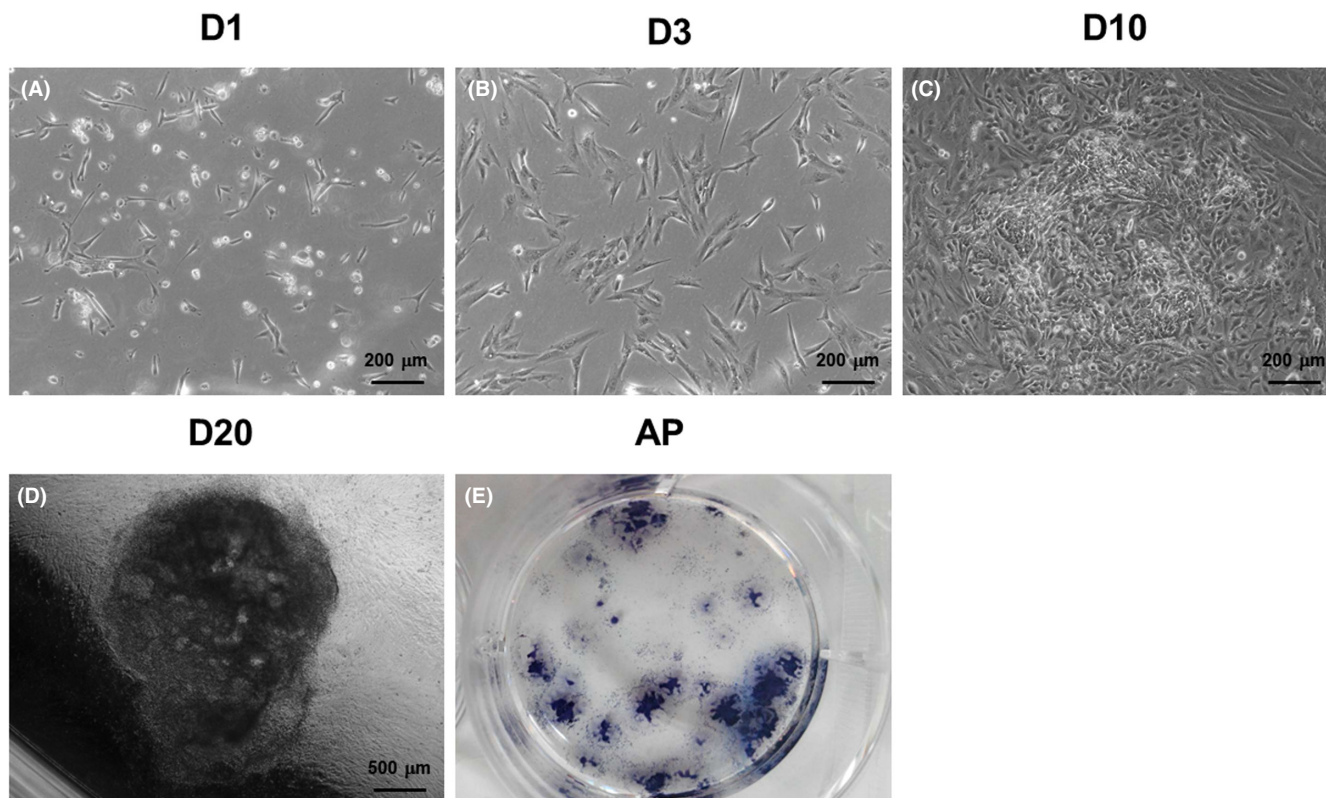
FIGURE 2 Cell morphology and AP staining during the induction of CV-iPSCs. (A-D) The cell morphology during the induction of iPSCs from CV cells in D1, D3, D10, and D20, respectively. Bar = 200 μm (A-C) or 500 μm (D). (E) AP staining of CV-iPSCs clones

higher compared with the 200 V + 100 μs (4.6%) and 200 V + 300 μs (23.7%) groups (Figure 1D). Based on the above findings, the EP condition of 200 V + 300 μs was applied to transfect CV cells to generate iPSCs.

## 3.2 | Cell morphology and AP staining during the transformation of CV cells into iPSCs

When reached ~70% confluency, CV cells were digested and counted. Both pEP4-E02S-ET2K and pCEP4-miR-302–367 plasmids were introduced into cells by EP at voltage pulse of 200 V for 300 μs. Since several cells were damaged and died due to EP, only few cells adhered to the wall on the second day after EP, while more dead cells were observed, resulting to a confluency of only ~10%, these cells defined as D1 cells (Figure 2A). On D3, cells were resulting to a confluency of only ~30% (Figure 2B). Following incubation into inducing medium for 10 days, dense cell clusters were observed, while cells exhibited short spindle or round morphology (Figure 2C). After culturing for ~20 days, typical ESC colonies began to appear, characterized by higher nucleus-to-cytoplasm ratio, tight and uniform cell arrangement, and clear, smooth and gradually expending clone edges (Figure 2D). At this time point, the cell clones were isolated, purified, and sub-cultured or stained with AP. Staining results showed that they were positive for AP (Figure 2E).

3.3 | Cell morphology of iPSC clones before and after passage

When the size of the iPSC-transformed typical ESC colonies occupied 1/2 of the microscope low-power field and had a particular thickness, the clones were isolated, purified, and sub-cultured using a mechanical method. When clones reached 50%–80% confluency with few differentiated cells, iPSCs were sub-cultured following digestion with EDTA. No differences were observed in iPSC morphology between cells purified by mechanical method (Figure 3A,B) and EDTA digestion (Figure 3C,A'). When reached 70%–90% confluency, iPSCs were cryopreserved using the programmed freezing method. The frozen cells were recovered using a quick-thawing method. However, no differences were observed in iPSC morphology prior freezing and after thawing (Figure 3B',C').

3.4 | Karyotype and non-integration analysis of primitive CV cells and CV-iPSCs

The karyotype analysis of primitive CV cells and CV-iPSCs after passage seven were detected. The results showed that CV-iPSCs exhibited the same normal karyotype as primitive CV cells (Figure 4A,B). Next, the absence of the reprogramming vectors were tested by PCR analysis and agarose gel electrophoresis, the results showed that the P2 of CV cells and the P11 of CV-iPSCs did not express
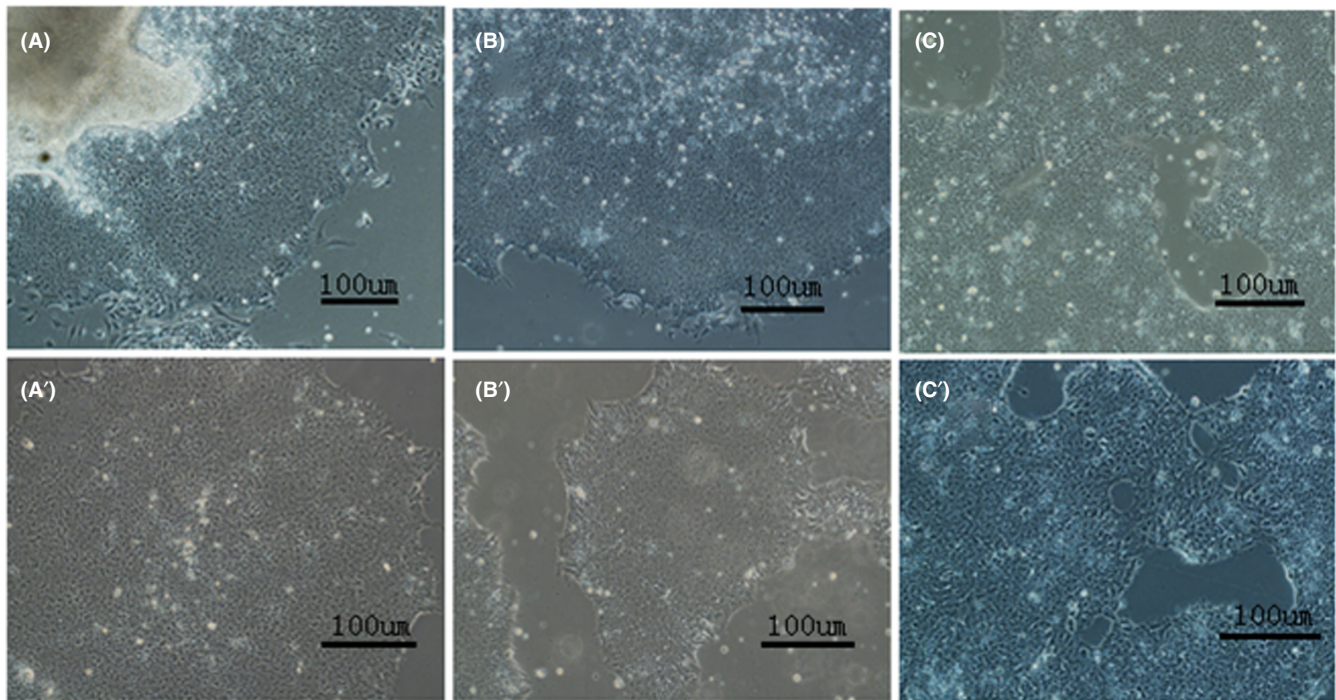
FIGURE 3 Morphology of CV-iPSCs. (A) The morphology of CV-iPSCs before mechanical purification. (B) The morphology of CV-iPSCs after mechanical purification. (C) The morphology of CV-iPSCs before the digestion method. (A') The morphology of CV-iPSCs after the digestion method (B') The morphology of CV-iPSCs before programmed freezing. (C') The morphology of CV-iPSCs after thawing culture

the exogenous genes SOX2, KLF4 OCT4, miR-302–367, orip, and EBNA-1 (Figure 4C), indicating that the plasmids were not integrated into the genomic DNA of CV-iPSCs cells, and the integrity of the genome was verified.

3.5 | Expression levels of pluripotency-related markers in CV-iPSCs

To evaluate the pluripotency of CV-iPSCs, the expression levels of the pluripotency-related markers OCT-4, SSEA-4, TRA-1–60, and TRA-1–81 were detected in CV-iPSCs using immunofluorescence staining. The results demonstrated that cells were positive for all the aforementioned markers (Figure 5A), thus indicating that CV-iPSCs exhibited the pluripotent features of iPSCs. RT-qPCR analysis further verified that the expression levels of SOX2, OCT4, and NANOG were significantly upregulated in CV-iPSCs compared with primitive CV cells (Figure 5B).

3.6 | Evaluation of the differentiation ability of CV-iPSCs

Since CV-iPSCs showed pluripotent characteristics in vitro, the current study aimed to further explore the differentiation ability of CV-iPSCs in vivo. Therefore, treated CV-iPSCs were subcutaneously injected into NOD-SCID mice. The results showed that all the three germ layers, namely the endoderm, the mesoderm, and the

ectoderm, were composed of the typical cells of the respiratory epithelium, adipose and cartilage tissues, and neuroepithelial cells, respectively (Figure 6).

4 | DISCUSSION

The iPSCs are considered as potential cell models for studying the regulation of cell differentiation,[19] disease pathogenesis,[8,20–24] organ regeneration,[25,26] stem cell therapy,[27–29] and drug screening.[30–34] Efficient and safe induction of CV cells is the key approach for the establishment and later application of iPSCs. The pEP4-E02S-ET2K plasmid, encompassing the human OCT4, S0X2, SV4 0LT, and KLF4 genes, used in the present study combined with the pCEP4-miR-302–367 plasmid, encompassing the miR-302/367 sequences, do not carry c-Myc oncogene, which exhibits carcinogenic effects. Therefore, c-Myc-mediated tumor formation and gene mutation are partially avoided,[35,36] while at the same time reprogramming efficiency can be improved.[37] In addition, four small molecule inhibitors were added during the induction process, thus further improving induction efficiency.[38–40]

In the present study, EP was used to transfer the aforementioned plasmids into cells, eventually avoiding the risk of integration into host genome.[14,15] However, the voltage electric pulse and the duration of the electric shock are key factors that affect the EP efficiency and the energy of the electric field. The greater the pulse voltage and the longer the duration, the greater the damage to the cells. Herein, using the same EP cup mode, CV cell transfection by EP at 200 V
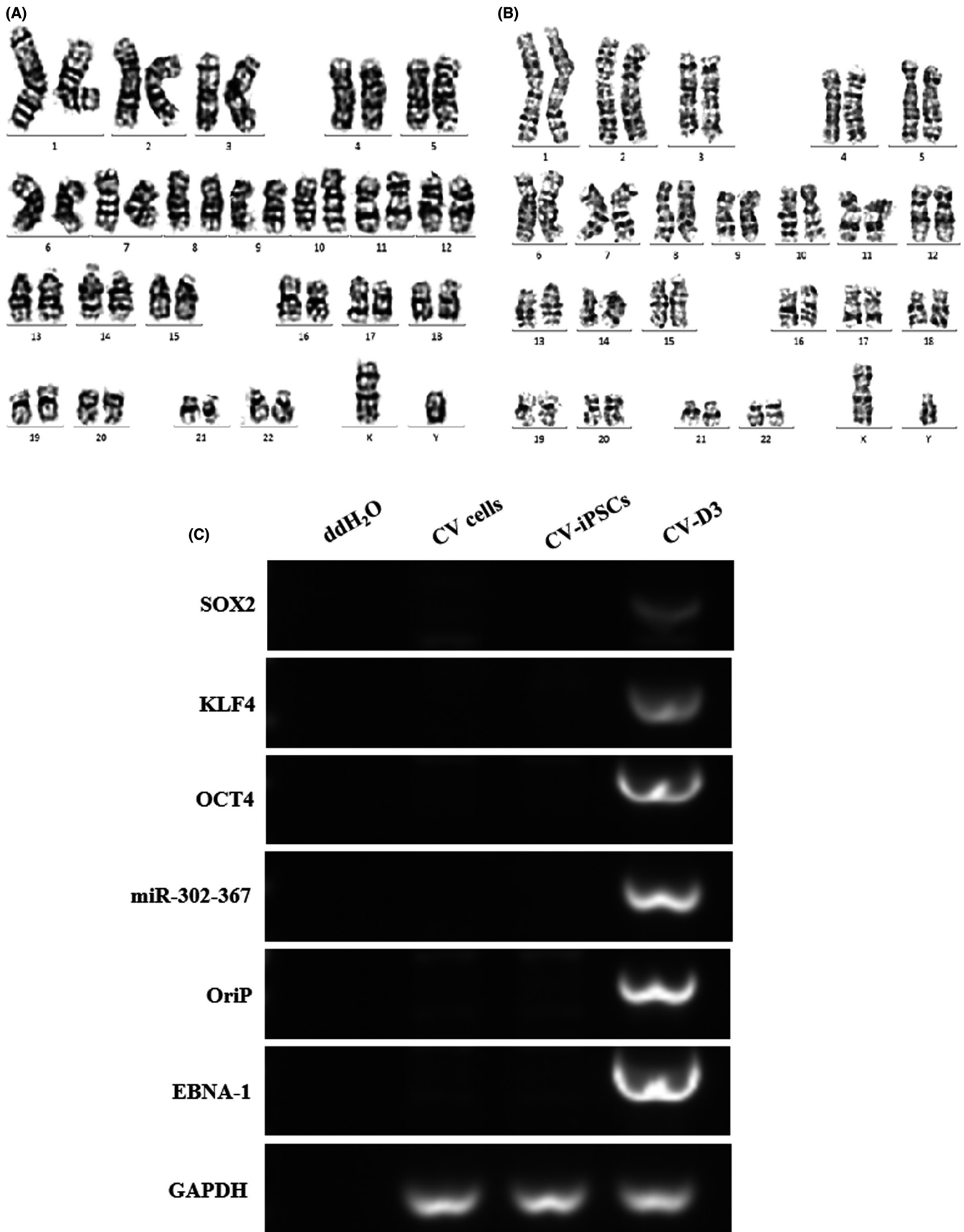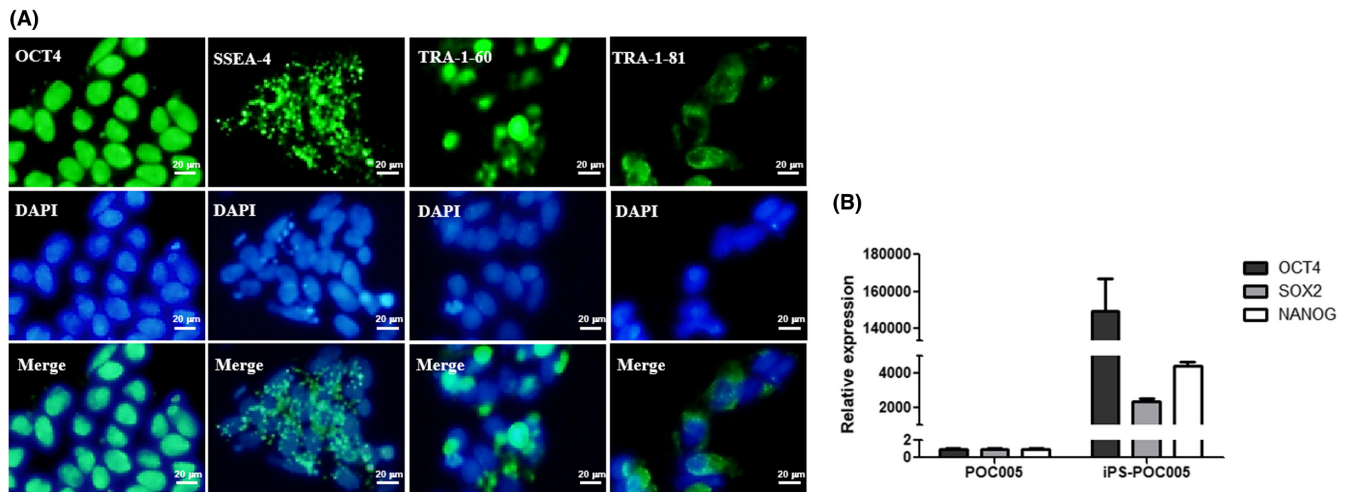
FIGURE 4 Karyotype and non-integration analysis. (A) The karyotype of primitive CV cells (cells before transfection). (B) The karyotype of CV-iPSCs after passage seven. (C) Non-integration analysis of CV cells and CV-iPSCs. The P2 CV cells and ddH₂O were regarded as negative control, and D3 cells after transfection (CV-D3) as positive control

(A)

(B)

FIGURE 5 Expression of pluripotent marker in CV-iPSCs. (A) The expression of pluripotent marker OCT4, SSEA4, TRA-1–60, and TRA-1–81 in CV-iPSCs by immunofluorescence staining (×1000). DAPI stained the nucleus (Blue). (B) The expression of pluripotent marker OCT4, SSEA4, TRA-1–60, and TRA-1–81 in CV-iPSCs by RT-qPCR
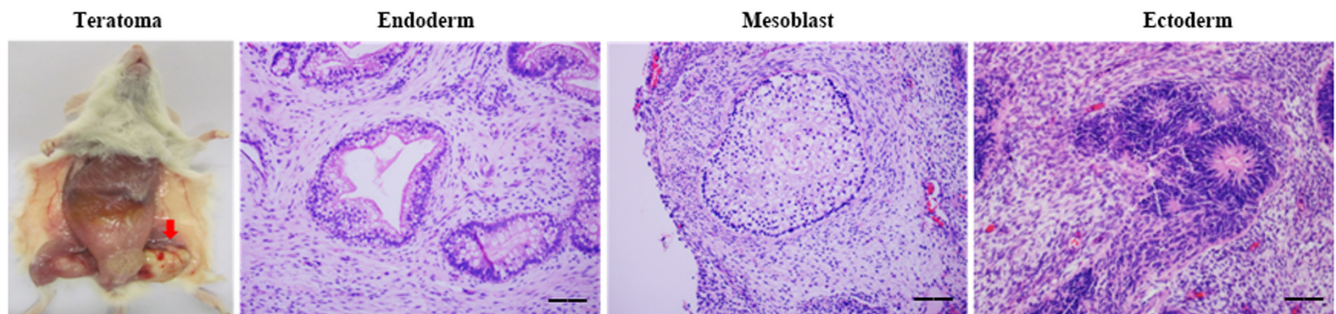
FIGURE 6 Teratoma formation of CV-iPSCs. Left: the view of mice anatomy. Right: the HE staining of typical cells of three germ layers endoderm, mesoderm, and ectoderm, respectively (×100)

for 300 µs showed higher cell transfection efficiency and survival rate. Although, the cell transfection efficiency in the 300 V + 300 µs EP group was higher, the cell survival rate was however reduced. Therefore, EP at 200 V for 300 µs with two electric shocks were recommended for the efficient transformation of human CV cells to iPSCs.

The isolated and purified CV-iPSCs were stably sub-cultured under the feeder- and serum-free culture system of Matrigel™ + mTeSR™1. CV-iPSCs showed a clone morphology similar to ESCs. Following continuous proliferation and sub-culture in vitro, CV-iPSCs maintained the same normal karyotype as the original CV cells and could consistently express the cell pluripotency markers OCT4, SSEA-4, TRA-1–60, and TRA-1–81. Additionally, cells showed positive AP staining, thus further supporting the pluripotency of CV-iPSCs. Furthermore, CV-iPSCs were injected into NOD-SCID mice resulting in the development of teratomas, thus suggesting that CV-iPSCs could differentiate into cells of all three germ layers.

In conclusion, the current study suggested that human CV cells could be transformed into non-integrated iPSCs exhibiting multidirectional differentiation potential. CV cell-derived iPSCs exhibited the same advantages with CV cells. On the one hand, CV cell-derived iPSCs can carry disease-specific genes, and therefore cell models from disease genotypes to phenotypes can be established in vitro. On the other hand, compared with cells derived from amniotic fluid, fetal skin fibroblasts, and lymphocytes, CV cells can be transformed into iPSCs in a shorter time, thus providing time for the autologous transplantation of fetal cells. Overall, these cells show irreplaceable advantages for their possible clinical application. Furthermore, the induction conditions selected in the present study could provide novel insights into the easy generation of iPSCs from CV cells and new directions for the further application of stem cells in clinical practice.

CONFLICT OF INTEREST

The authors declare no conflict of interest.

AUTHOR CONTRIBUTIONS

MYL conceived and supervised the research and its design. LP and JQL designed and performed the experiments, interpreted the data, and wrote the article. SYC, SF, WYJ, WBY, and LQ assigned reagents/materials/analytical tools. All authors approved the final article.

DATA AVAILABILITY STATEMENT

The data that support the findings of this study are available from the corresponding author upon reasonable request.

ORCID

Qiuling Jie https://orcid.org/0000-0002-1338-0888
Yanlin Ma https://orcid.org/0000-0001-9668-0204

REFERENCES

1. Takahashi K, Yamanaka S. Induction of pluripotent stem cells from mouse embryonic and adult fibroblast cultures by defined factors. *Cell.* 2006;126(4):663-676.
2. Takahashi K, Tanabe K, Ohnuki M, et al. Induction of pluripotent stem cells from adult human fibroblasts by defined factors. *Cell.* 2007;131(5):861-872.
3. Jacków J, Guo Z, Hansen C, et al. CRISPR/Cas9-based targeted genome editing for correction of recessive dystrophic epidermolysis bullosa using iPS cells [published online ahead of print, 2019 Dec 9]. *Proc Natl Acad Sci USA.* 2019;116(52):26846-26852.
4. Sun N, Panetta NJ, Gupta DM, et al. Feeder-free derivation of induced pluripotent stem cells from adult human adipose stem cells. *Proc Natl Acad Sci USA.* 2009;106(37):15720-15725.
5. Su RJ, Neises A, Zhang XB. Generation of iPS cells from human peripheral blood mononuclear cells using episomal vectors. *Methods Mol Biol.* 2016;1357:57-69.
6. Shaw SWS, Cheng PJ, Chang YL, et al. Human amniotic fluid stem cells have better potential in early second trimester of pregnancy and can be reprogramed to iPS. *Taiwan J Obstet Gynecol.* 2017;56(6):770-774.
7. Gaignerie A, Lefort N, Rousselle M, et al. Urine-derived cells provide a readily accessible cell type for feeder-free mRNA reprogramming. *Sci Rep.* 2018;8(1):14363.
8. Wei Y, Zhou X, Huang W, et al. Generation of trophoblast-like cells from the amnion in vitro: a novel cellular model for trophoblast development. *Placenta.* 2017;51:28-37.
9. Cai J, Li W, Su H, et al. Generation of human induced pluripotent stem cells from umbilical cord matrix and amniotic membrane mesenchymal cells. *J Biol Chem.* 2010;285(15):11227-11234.
10. Ye L, Chang JC, Lin C, Sun X, Yu J, Kan YW. Induced pluripotent stem cells offer new approach to therapy in thalassemia and sickle cell anemia and option in prenatal diagnosis in genetic diseases. *Proc Natl Acad Sci USA.* 2009;106(24):9826-9830.
11. Lichtner B, Matz P, Adjaye J. Generation of iPSC lines from primary human chorionic villi cells. *Stem Cell Res.* 2015;15(3):697-699.
12. Zhu X, Cai A, Meng J, et al. Generation of ZZUi008-A, a transgene-free, induced pluripotent stem cell line derived from chorionic villi

cells of a fetus with Duchenne muscular dystrophy. *Stem Cell Res.* 2018;32:47-50.
13. Parveen S, Panicker MM, Gupta PK. Generation of an induced pluripotent stem cell line from chorionic villi of a Turner syndrome spontaneous abortion. *Stem Cell Res.* 2017;19:12-16.
14. Gore A, Li Z, Fung HL, et al. Somatic coding mutations in human induced pluripotent stem cells. *Nature.* 2011;471(7336):63-67.
15. Araki R, Mizutani E, Hoki Y, et al. The number of point mutations in induced pluripotent stem cells and nuclear transfer embryonic stem cells depends on the method and somatic cell type used for their generation. *Stem Cells.* 2017;35(5):1189-1196.
16. Luft C, Ketteler R. Electroporation knows no boundaries: the use of electrostimulation for sirna delivery in cells and tissues. *J Biomol Screen.* 2015;20(8):932-942.
17. Deora AA, Diaz F, Schreiner R, Rodriguez-Boulan E. Efficient electroporation of DNA and protein into confluent and differentiated epithelial cells in culture. *Traffic.* 2007;8(10):1304-1312.
18. Xue Y, Cai X, Wang L, et al. Generating a non-integrating human induced pluripotent stem cell bank from urine-derived cells. *PLoS One.* 2013;8(8):e70573.
19. Soufi A, Garcia MF, Jaroszewicz A, Osman N, Pellegrini M, Zaret KS. Pioneer transcription factors target partial DNA motifs on nucleosomes to initiate reprogramming. *Cell.* 2015;161(3):555-568.
20. Cereso N, Pequignot MO, Robert L, et al. Proof of concept for AAV2/5-mediated gene therapy in iPSC-derived retinal pigment epithelium of a choroideremia patient. *Mol Ther Methods Clin Dev.* 2014;1:14011.
21. Farkhondeh A, Li R, Gorshkov K, et al. Induced pluripotent stem cells for neural drug discovery. *Drug Discov Today.* 2019;24(4):992-999.
22. Itzhaki I, Maizels L, Huber I, et al. Modelling the long QT syndrome with induced pluripotent stem cells. *Nature.* 2011;471(7337):225-229.
23. Adami R, Bottai D. Spinal muscular atrophy modeling and treatment advances by induced pluripotent stem cells studies. *Stem Cell Rev Rep.* 2019;15(6):795-813.
24. Marchetto MC, Carromeu C, Acab A, et al. A model for neural development and treatment of Rett syndrome using human induced pluripotent stem cells. *Cell.* 2010;143(4):527-539.
25. Turco MY, Gardner L, Kay RG, et al. Trophoblast organoids as a model for maternal-fetal interactions during human placentation. *Nature.* 2018;564(7735):263-267.
26. Vegas AJ, Veiseh O, Gürtler M, et al. Long-term glycemic control using polymer-encapsulated human stem cell-derived beta cells in immune-competent mice [published correction appears in Nat Med. 2016 Apr;22(4):446]. *Nat Med.* 2016;22(3):306-311.
27. Tolosa L, Caron J, Hannoun Z, et al. Transplantation of hESC-derived hepatocytes protects mice from liver injury. *Stem Cell Res Ther.* 2015;6:246.
28. Fatehullah A, Tan SH, Barker N. Organoids as an in vitro model of human development and disease. *Nat Cell Biol.* 2016;18(3):246-254.
29. Mandai M, Watanabe A, Kurimoto Y, et al. Autologous induced stem-cell-derived retinal cells for macular degeneration. *N Engl J Med.* 2017;376(11):1038-1046.
30. Liang P, Lan F, Lee AS, et al. Drug screening using a library of human induced pluripotent stem cell-derived cardiomyocytes reveals disease-specific patterns of cardiotoxicity. *Circulation.* 2013;127(16):1677-1691.
31. Deguchi S, Yamashita T, Igai K, et al. Modeling of hepatic drug metabolism and responses in CYP2C19 poor metabolizer using genetically manipulated human iPS cells. *Drug Metab Dispos.* 2019;47(6):632-638.
32. Naryshkin NA, Weetall M, Dakka A, et al. Motor neuron disease. SMN2 splicing modifiers improve motor function and longevity in mice with spinal muscular atrophy. *Science.* 2014;345(6197):688-693.

33. Burkhardt MF, Martinez FJ, Wright S, et al. A cellular model for sporadic ALS using patient-derived induced pluripotent stem cells. *Mol Cell Neurosci*. 2013;56:355-364.

34. Ikeda K, Kawasaki Y, Matsuda H, et al. Approach for differentiating trophoblast cell lineage from human induced pluripotent stem cells with retinoic acid in the absence of bone morphogenetic protein 4. *Placenta*. 2018;71:24-30.

35. Pera MF. Stem cells: the dark side of induced pluripotency. *Nature*. 2011;471(7336):46-47.

36. Kilpinen H, Goncalves A, Leha A, et al. Common genetic variation drives molecular heterogeneity in human iPSCs [published correction appears in Nature. 2017 Jun 29;546(7660):686]. *Nature*. 2017;546(7658):370-375.

37. Anokye-Danso F, Trivedi CM, Juhr D, et al. Highly efficient miRNA-mediated reprogramming of mouse and human somatic cells to pluripotency [published correction appears in Cell Stem Cell. 2012 Dec 7;11(6):853]. *Cell Stem Cell*. 2011;8(4):376-388.

38. Li D, Wang L, Hou J, et al. Optimized approaches for generation of integration-free iPSCs from human urine-derived cells with small molecules and autologous feeder. *Stem Cell Rep*. 2016;6(5):717-728.

39. Liu G, David BT, Trawczynski M, Fessler RG. Advances in pluripotent stem cells: history, mechanisms, technologies, and applications. *Stem Cell Rev Rep*. 2020;16(1):3-32.

40. Omole AE, Fakoya AOJ. Ten years of progress and promise of induced pluripotent stem cells: historical origins, characteristics, mechanisms, limitations, and potential applications. *PeerJ*. 2018;6:e4370.